

QUASI-NEWTON MODEL-TRUST REGION APPROACH TO SURROGATE-BASED OPTIMISATION OF PLANAR METAMATERIAL STRUCTURES

Patrick J. Bradley*

RF & Microwave Research Group, School of Electrical Electronic and Communications Engineering, University College Dublin, Ireland

Abstract—A novel implementation of aggressive space mapping (ASM) for the automatic layout synthesis of planar metamaterial structures is outlined in this article. Specifically, we employ a model-trust region optimisation approach to significantly reduce the computational burden associated with the direct optimisation of high-fidelity models. A Visual Basic for application (VBA) link to a commercial full-wave electromagnetic (EM) solver is created, to ensure that the automated Matlab-based platform has complete control of the design and analysis of the entire ASM process. The validity and efficiency of our approach is demonstrated with examples of complementary split-ring resonator (CSRR)-loaded transmission lines, comparing both modified and unmodified version of the quasi-Newton iteration within the ASM framework.

1. INTRODUCTION

Automatic synthesis of RF and microwave circuits remains a critical step in computer-aided design. Although numerous optimisation processes exist for full-wave EM simulators, they are plagued by the high computational cost of directly optimising high-fidelity (fine) models. With the advent of space mapping (SM) and surrogate based optimisation, this major bottleneck was removed, by replacing the full-wave model with a low-fidelity (coarse) model [1–3]. The SM technique aligns the coarse model with the fine model in an iterative optimisation process, where most of the burden of the multiple system analysis is placed on the coarse model.

In Bandler's seminal paper [4], he presents a significantly improved approach to SM, employing a quasi-Newton iteration in

Received 5 October 2012, Accepted 7 December 2012, Scheduled 10 December 2012

* Corresponding author: Patrick J. Bradley (patrick.bradley@ucd.ie).

conjunction with first-order derivative approximations updated by the classic Broyden formula [5]. SM exploits physically-based coarse models, typically equivalent circuits of the microwave structure under consideration. This allows the SM algorithm to yield satisfactory results after a few fine model evaluations. However, reliable equivalent circuit models may be difficult to develop for certain types of microwave devices. Moreover, even if only a few iterations of the SM algorithm are needed, the repeated simulation of the fine model may still be too computationally prohibitive. Quasi-Newton techniques for minimisations are popular, particularly whenever the matrix-valued second derivative of the objective function is not known analytically or is prohibitively expensive to compute. Unfortunately, it is not unusual to expend significant computational effort in getting an optimum solution using a basic quasi-Newton approach.

Quasi-Newton methods, like all Newton-like methods, must be augmented with auxiliary procedures that increase the likelihood of convergence to a solution, when good initial approximate solutions are not available. There are two major augmentations that can be implemented, backtracking line-search methods, in which step lengths are adjusted to obtain satisfactory steps, and model-trust region methods, in which a step is ideally chosen to minimize the norm of the local linear model within a specified trust region. Backtracking line-search methods are relatively easy to implement. However, each step direction is restricted to be that of the initial trial step. While this step is normally constructed to be a descent direction, it may be only a weak descent direction, especially if the Jacobian is ill-conditioned [5]. Since model-trust region steps are increasingly in the steepest-descent direction as the model-trust region radius decreases, these methods have the potential advantage of producing modified steps. However, their implementation in practical methods may be problematic [6].

Model-trust region inspired space mapping approaches were first pioneered by [7] and more recently [3] has refined this approach for microwave structures. For the purpose of the automated synthesis of planar metamaterial structures, by building on the work of [8], we have designed a flexible and efficient optimisation technique based on the model-trust region algorithm that has been adapted for the optimisation of a CSRR-loaded transmission line. The resulting algorithm incorporates a reliable parameter extraction step critical to the convergence of the technique and includes a comprehensive series of procedures to ensure a robust implementation. In addition, we also endeavored to create a fully automated and versatile software platform. To this end, we employed a Visual Basic for application (VBA) link to create a interface with our full-wave EM solver, ensuring that the

automated Matlab-based platform has complete control of the design and analysis of the entire ASM process.

2. AGGRESSIVE SPACE MAPPING IMPLEMENTATION

The basic structure under study is a complementary split-ring resonator (CSRR)-loaded transmission line with CSRRs etched in the ground plane as shown in Figure 1(a). As discussed in [9, 10], CSRRs behave as electrical dipoles that can be excited by axial electric fields and exhibit negative permittivity upon their resonance. Typically CSRRs are used for the synthesis of compact planar filters or to improve the performance of existing ones.

Due to the small electrical dimension of CSRRs at resonance, the unit cell can be described by means of a lumped-element equivalent

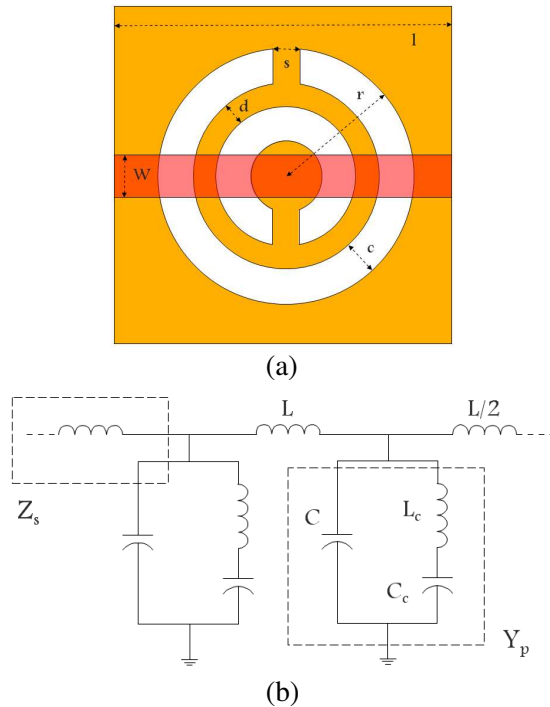


Figure 1. (a) Topology of the CSRR loaded transmission line for a single unit periodic structure and (b) the simplified lumped element equivalent circuit model for two unit periodic structure where Z_s and Z_p are the series and shunt impedance of the T-circuit model repetitively.

circuit, Figure 1(b), where L and C are the per-unit-cell inductance and capacitance of the host line. CSRRs are modelled as a resonant tank (L_c, C_c) electrically coupled to the line through C_m [11]. In order to infer a relationship between the response of the full-wave simulator and the circuit model, three distinct characteristic frequencies must be identified [9, 10, 12]; the transmission zero frequency f_z , the reflection zero frequency f_0 , and the frequency f_p providing -90° phase shift for S_{21} . Based on these characteristic frequencies, and after some derivation, we can arrive at the following expression for the lumped elements [11]

$$L_c = \frac{-(L\omega_p^2(\omega_p^2 - \omega_z^2))}{((\omega_o^2 - \omega_p^2)(\omega_0^2 - \omega_z^2))} \quad (1)$$

$$C_c = 1/(\omega_0^2 L_c) \quad (2)$$

while L, C can be calculated from traditional transmission line equations [13][†].

The ASM methodology exploits underlying fast-to-compute, low-fidelity models that can validate high-fidelity designs when classical optimisation algorithms are impracticable. Formally, the goal of the ASM is to solve

$$\mathbf{x}_f^* = \arg \min f(\mathbf{r}(\mathbf{x}_f)) \quad (3)$$

where f is the objective function given by

$$f(\mathbf{r}(\mathbf{x}_f)) = \|\mathbf{r}(\mathbf{x}_f)\|_2 = \|\mathbf{y}_c^* - P(\mathbf{x}_f)\|_2 \quad (4)$$

and $P(\mathbf{x}_f) = \mathbf{y}_f = [L_c, C_c, L, C]$ is the extracted model parameters obtained from the EM response. The solution of which, will generate an optimum set of geometry values \mathbf{x}_f^* , that approximate the optimum response of the low fidelity model $\mathbf{y}_c^* = [L_c^*, C_c^*, L^*, C^*]$ (the subscript f and c refer to the fine and course models respectively).

The ASM algorithm, as outlined in Appendix A, is essentially a construction of four main modules; a module for the determination of the initial geometry $\mathbf{x}_f = [r, d, w, c]$, a link to a EM solver that provides the fine model response (S -parameters), a parameter extraction module that determines the model parameters from the EM response $P(\mathbf{x}_f)$, and an optimisation algorithm that provides the next set of geometry parameters. In order to characterise the initial CSRR dimensions, we employ expressions given in [9, 14]. This approach requires fixing c, s (the CSRRs ring width, split width) to a reasonable value and linking the transmission line length l to r (the CSRRs

[†] Due to hyper-sensitivity of the reflection zero frequency to small variations in the geometry it is recommended to using traditional transmission line equations to extract the electrical parameters L, C so as to ensure a stable ASM algorithm.

outer radius), in order to univocally determine the initial geometry. To obtain the transmission line width w , classical expressions for the characteristic impedance are used [13,15], based on L and C . From the initial full-wave EM response based on \mathbf{x}_f^1 , we extract the circuit parameters $P(\mathbf{x}_f)$ using Equation (2), in order to obtain the objective function f .

To achieve fast convergence, the Broyden quasi-Newton approach requires the initial iterative to be in the neighborhood of the solution but it is also dependant on a good choice of \mathbf{J}^1 , the initial Jacobian approximation. This approximation must attempt to be close to the true Jacobian at the solution $\mathbf{J}(\mathbf{x}_f^*)$, therefore setting $\mathbf{J}^1 = \mathbf{J}(\mathbf{x}_f^1)$ is a prudent choice. This is achieved by observing the changes in $P(\mathbf{x}_f)$ values in response to small perturbations in the geometry variables \mathbf{x}_f^1 using the forward-difference formula.

Although most commercial EM solver programs now come with some numerical optimisation, they lack the versatility of optimisation routines that are available within Matlab. The powerful analysis tools available in Matlab make it a ideal platform for the design, analysis and control of a Matlab-based ASM software system that can be interfaced with a EM simulator to provide a fully automatic looped optimisation process. In this paper, we use a VBA link to create a interface with CST Microwave Studio[‡], but a similar approach can be implemented for Ansoft HFSS, while COMSOL provides live-link functionality for Matlab.

3. MODEL-TRUST REGION

Model-trust region methods are heuristic procedures, that combine the strengths of both the steepest-descent method and the quasi-Newton method [5,16]. The steepest-descent method guarantees progress toward the goal of a local minimum. However, if the solution landscape is not well-conditioned, it will take a long time for the program to reach the final goal. The quasi-Newton method, on the other hand, converges quickly in the vicinity of a local minimum, but can diverge or cycle when starting far from a local minimum [5]. This combined approach guarantees convergence to a local minimum from any starting search point by searching in a direction that interpolates between steepest-descent (Cauchy) and the quasi-Newton direction. Favoring steepest-descent when progress is slow and moving to quasi-Newton as progress improves.

[‡] Due to the high Q nature of the outlined structure a time step stability factor of < 1 is recommended.

The model-trust region methods produce a trial step by minimising a quadratic model of the objective function subject to a constraint on the length of the trial step to a restricted ellipsoidal region [17]. The diameter of this region is expanded and contracted in a controlled way based upon how well the local model predicts behavior of the objective function. At each iteration of a model-trust region method, the objective function f is replaced by a quadratic model of $f(\mathbf{x}_k)$ centered on the current iterate k , denoted by

$$m_k(\mathbf{x}_k + \mathbf{s}) = f(\mathbf{x}_k) + \mathbf{s}^T \nabla f(\mathbf{x}_k) + \frac{1}{2} \mathbf{s}^T \mathbf{H}_k \mathbf{s} = f(\mathbf{x}_k) + \mathbf{s}^T \mathbf{J}^T \mathbf{r} + \frac{1}{2} \mathbf{s}^T \mathbf{J}^T \mathbf{J} \mathbf{s} \quad (5)$$

where $\mathbf{H}_k = \mathbf{J}^T \mathbf{J}$ is used as the approximate Hessian in the model function and \mathbf{J} is the approximate Jacobian [8]. The model function is trusted to accurately represent f only from points with a sphere of radius δ centred on the current point. A candidate for the next iterative is then yielded by solving a sequence of subproblems in which the model is appropriately minimised with the model-trust region

$$\min m_k(\mathbf{x}_k + \mathbf{s}) \quad \text{subject to } \|\mathbf{s}\| \leq \delta. \quad (6)$$

Although principally we seek the optimal solution of Equation (6), it is enough for the purpose of global convergence to find an approximate solution that lies within the trust region and gives a sufficient reduction in the model. A simple strategy is to minimise the model along the steepest-descent direction $-\mathbf{J}^T \mathbf{r}_k$, subject to the model-trust region bound. However, it has been shown that this approach has a unacceptably slow rate of convergence. To improve the convergence speed in the terminal phase we must allow for approximations in the quasi-Newton direction. The double dogleg technique is such a method, that approximates the solution of the model-trust region problem by minimising m_k along a piecewise linear path [17]. When δ is small, \mathbf{x}_{k+1} is more in the direction of the steepest-descent direction $\mathbf{s}^c = -\lambda \mathbf{J}_c^T \mathbf{r}_c$, and moves in the direction of the quasi-Newton direction as the model-trust region radius increases.

The Cauchy point is defined by the unconstrained minimiser of the objective function along the steepest descent direction and given by $\mathbf{s}^c = -\lambda \mathbf{J}_c^T \mathbf{r}_c$, where

$$\lambda = \frac{(\|\mathbf{J}_c^T \mathbf{r}_c\|_2^2)}{((\mathbf{J}_c^T \mathbf{r}_c)^T (\mathbf{J}^T \mathbf{J}) \mathbf{J}_c^T \mathbf{r}_c)}. \quad (7)$$

The line segment connecting the Cauchy point to the quasi-Newton direction is parameterised by

$$\mathbf{x}_{k+1}(\tau) = \mathbf{x}_k + \mathbf{s}^c + \tau(\eta \mathbf{s}^n - \mathbf{s}^c) \quad 0 \leq \tau \leq 1 \quad (8)$$

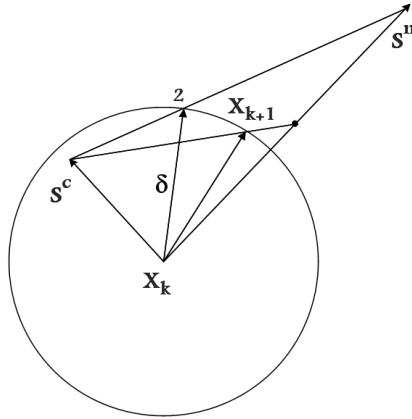


Figure 2. The single (point 2) and double dogleg paths \mathbf{x}_{k+1} .

where τ is calculated to ensure \mathbf{x}_{k+1} is on the curve such that $\|\mathbf{s}\|_2 = \delta$. An original choice of $\eta = 1$, results in the single dogleg [18], as shown in Figure 2 (point 2). In the double dogleg strategy, where $\eta = 0.8\gamma + 0.2$, better performance was observed by introducing a bias towards the quasi-Newton direction [6, 19].

Once a new point has been decided, a check must be performed to ensure that this step is satisfactory, that is to say that the new point will ensure a sufficient decrease in the objective function f . The condition to accept \mathbf{x}_{k+1} is based on [17]

$$f(\mathbf{x}_{k+1}) \leq f(\mathbf{x}_k) + \alpha(\mathbf{J}\mathbf{r}_k)^T \mathbf{s} \tag{9}$$

where $(\mathbf{J}\mathbf{r}_k)^T$ is an approximation to $\nabla f(\mathbf{x}_k)$, and α is a constant chosen to be 10^{-4} . This step-acceptance criteria requires that the rate of decrease from $f(\mathbf{x}_k)$ to $f(\mathbf{x}_{k+1})$ be at least some fraction α of the initial rate of decrease in that direction. If \mathbf{x}_{k+1} is unacceptable we reduce the model-trust region and minimise the same quadratic model on the smaller model-trust region. The model-trust region is reduced by a factor λ , between upper and lower heuristic safeguards of 0.5 and 0.1, and returned to the approximate solution of the minimisation problem by the double dogleg method. The reduction factor is determined by finding the minimiser of a quadratic that models $f(\mathbf{x}_k + \lambda\mathbf{s})$, which occurs at

$$\lambda = - \frac{(\mathbf{J}\mathbf{r}_k)^T \mathbf{s}}{2 \left(f(\mathbf{x}_{k+1}) - f(\mathbf{x}_k) - (\mathbf{J}\mathbf{r}_k)^T \mathbf{s} \right)}. \tag{10}$$

The model-trust region radius is then set to $\delta = \lambda$ unless $\lambda \in$

$[0.1\delta, 0.5\delta]$, where instead λ is set to the closer endpoint of the safeguard interval [17]. These safeguards are in place to ensure that the model-trust region radius is not inadvertently decreased by an aggressive amount based on a poorly modelled quadratic in this region. However, if the new iterative is satisfactory, we must then decide whether the model-trust region should be changed. We base this choice on the agreement between the model function m_k and the objective function f at previous iterations. Given a step \mathbf{s} , we compare the ratio of the actual reduction $\Delta f_{act} \equiv f(\mathbf{x}_{k+1}) - f(\mathbf{x}_k)$ to the predicted reduction by the model function $\Delta f_{pre} \equiv m_k(\mathbf{x}_{k+1}) - f(\mathbf{x}_k)$

$$\rho = (f(\mathbf{x}_{k+1}) - f(\mathbf{x}_k)) / \left((\mathbf{J}\mathbf{r}_k)^T \mathbf{s} + 0.5\mathbf{s}^T (\mathbf{J}^T \mathbf{J}) \mathbf{s} \right). \quad (11)$$

If there is a good agreement between the current quadratic model and the objective function ($\rho \geq 0.75$) then we can safely double the trust region radius at the next iteration. However, if the model has overestimated the decrease in the objective function ($\rho \leq 0.1$) then we shrink the radius by half, otherwise the model-trust region is kept unaltered.

As an additional step to improve the convergence of the model-trust region method, measures should be put in place to aggressively increase the trust region radius if the proceeding iteration was very successful. In this case, we may consider computing a larger step using the current model with a doubled model-trust region radius. This may be justified by the need to avoid a situation where the model-trust region has contracted, and now needs to be increased rapidly having entered a region where the function is better approximated, avoiding the need for unnecessary small step sizes. This approach of internal doubling [17] is particularly useful as a safeguard when the algorithm may start to converge to a point that looks like a local minimiser but then finds a way out, and requires a rapid increase in the model-trust region to recover the algorithm. The decision to justify an internal doubling is based on the previous principle of comparing the actual reduction to the predicted,

$$\|f_{pre} - f_{act}\|_2 \leq 0.1 \|f_{act}\|_2. \quad (12)$$

In this case, δ is an underestimate of the radius in which the model m adequately represents f , and therefore we need to double δ and compute a new \mathbf{x}_{k+1} , using the current model. However if the new step is unsuccessful we then step back to the previous computed step.

4. RESULTS

In order to demonstrate the efficiency and robustness of the model-trust space implementation of the ASM synthesis technique, we apply

it to the determination of the geometric parameters for a single and periodic CSRR loaded transmission line structure.

4.1. Case Study A

Following the procedure outlined in the previous sections the optimised electrical target parameters ($\mathbf{y}_c^* = [L_c = 6.76 \text{ nH}, C_c = 0.97 \text{ pF}, L = 4.47 \text{ nH}, C = 2.63 \text{ pF}]$)[§] are first obtained using a circuit simulator. This in turn provides us with the initial layout for the full-wave EM simulator ($\mathbf{x}_f^1 = [r = 4.18 \text{ mm}, d = 0.2 \text{ mm}, w = 1.6 \text{ mm}, c = 0.20 \text{ mm}]$), the transmission line length is contained to $l = 3r$, the split gap $s = 0.07r$, while a Taconic CER-10 substrate is employed with a thickness of 1.27 mm and dielectric constant $\epsilon_r = 10$ (of course, if the circuit parameters are extreme it might not be possible to generate a physical layout. Limited design guidelines for CSRR-loaded lines are available, and should be used to provide some useful intervals over which CSRRs can be used [20]).

Given these initial parameters we now compare the effectiveness of the model-trust space ASM algorithm to a unmodified quasi-Newton algorithm. A decision on convergence is based on testing whether \mathbf{x}_{k+1} approximately solves our optimisation problem, that is if $f(\mathbf{x}_{k+1}) \leq (\text{tol} = 0.05)$. In this case, convergence is achieved after 3 steps of the unmodified Quasi-Newton iteration and 5 steps of the model-trust space implementation, Figures 3(a), 3(b). All the requirements needed to achieve a quadratic convergence were evident in the example, the solution landscape was well-conditioned, as highlighted by the contour plot of Figure 4(a), the initial Jacobian was a good approximation to the true Jacobian at the solution $\mathbf{J}(\mathbf{x}_f^*)$, and the initial iterative was in the neighborhood of the solution. Although the model-trust approach was slower to converge, its internal doubling safeguards, as discussed in Section 3, insured that only two extra steps were required to achieve convergence.

The resulting circuit parameters after convergence are ($P(\mathbf{x}_f^5) = [L_c = 6.74, C_c = 0.97, L = 4.47, C = 2.63]$), with corresponding geometric optimised values of $\mathbf{x}_f^8 = [r = 3.97 \text{ mm}, d = 0.25 \text{ mm}, w = 1.87 \text{ mm}, c = 0.17 \text{ mm}]$. These results, as depicted in Figure 4(b), show both the agreement with the target response and the discrepancies of the initial layout parameters ($P(\mathbf{x}_f^1) = [L_c = 8.71, C_c = 0.82, L = 5.05, C = 2.51]$).

[§] Note that the electrical parameters are given in nH and pF so as to prevent any scaling issues within the modified quasi-Newton algorithm.

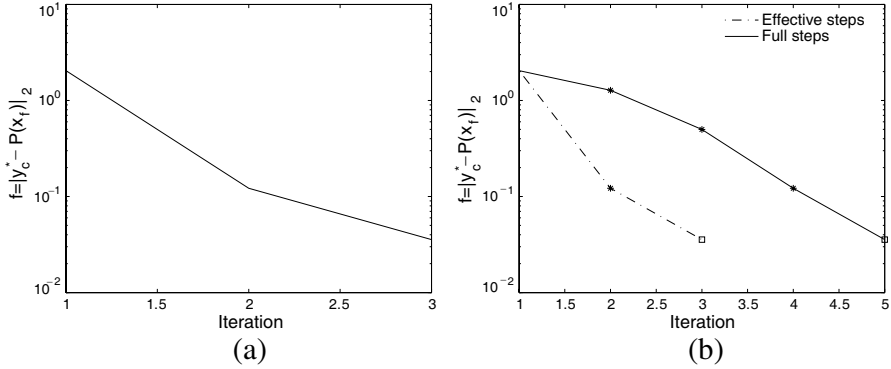


Figure 3. (a) The unmodified quasi-Newton iteration and (b) model-trust space iteration illustrating both the objective function values before and after refinement.

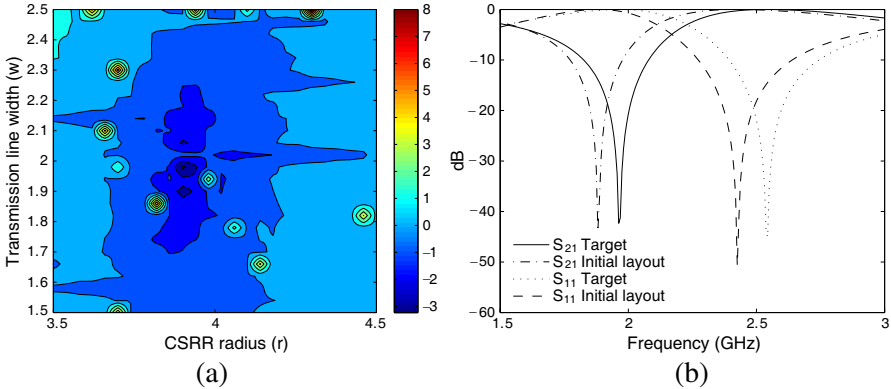


Figure 4. (a) Contour plot of the log (objective function values) over a range of r and w values using the optimum values for c and d and (b) transmission and reflection coefficient for the initial and final solution of a single-unit periodic CSRR-loaded transmission line.

4.2. Case Study B

The initial example clearly shows how all the requirements for a successful quasi-Newton approach are adhered to. Thus an ASM utilising this approach can be very effective. However, when operating with a less well-defined space (Figure 6(b)), taking large unconstrained steps within the solution landscape, can result in the iteration getting caught in a false minimum. In this example, we will show that by taking measured controlled steps whose direction can be modified,

these effects can be mitigated and will result in a significantly more robust ASM optimisation algorithm.

The target response was given from the design specifications of a two-unit periodic CSRR loaded transmission device with total length of $2l$ and are given by ($\mathbf{y}_c^* = [L_c = 10.9 \text{ nH}, C_c = 0.26 \text{ pF}, L = 4.25 \text{ nH}, C = 1.53 \text{ pF}]$) and ($\mathbf{x}_f^1 = [r = 2.5 \text{ mm}, d = 0.21 \text{ mm}, w = 1.08 \text{ mm}, c = 0.20 \text{ mm}]$). As before we use a Taconic CER-10 substrate with a thickness of 1.27 mm, dielectric constant $\epsilon_r = 10$, split gap $s = 0.07r$ and the transmission line length is contained to $l = 3r$. Based on these conditions we compare the effectiveness of the model-trust space ASM algorithm to a unmodified quasi-Newton algorithm and a modified Quasi-Newton with a backtracking line-search procedure [17]. To safeguard against stagnation a maximum of 3 backtrack steps were enforced in the implemented line-search quasi-Newton approach.

Unlike the previous case the unmodified quasi-Newton approach, Figure 5(a), and the modified approach with backtracking line-search, Figure 5(b), fails to converge with the more difficult solution space. It is evident, that the model-trust region method, Figure 6(a), converges to a norm of 0.048 at iteration 8. However, after step 3 the model-trust region radius is reduced 5 times with a double dogleg step taken on each occasion. On the penultimate step, the radius remains unaltered and a Cauchy step is subsequently taken which triggers the stop criteria.

The difficulties encountered by the line search algorithm are negated with the model-trust region method by overcoming two central problems. The first issue is the need to retain the same step direction regardless if this quasi-Newton step is unsatisfactory, and secondly the ability to transition smoothly between the steepest-descent direction

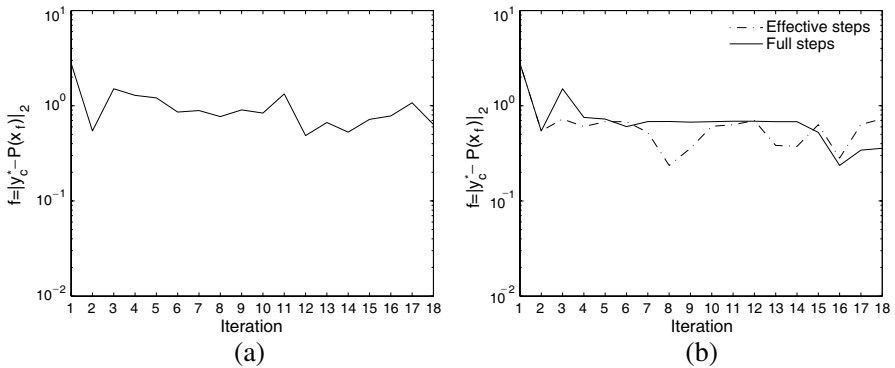


Figure 5. (a) The unmodified quasi-Newton iteration and (b) modified quasi-Newton iteration with backtracking line search.

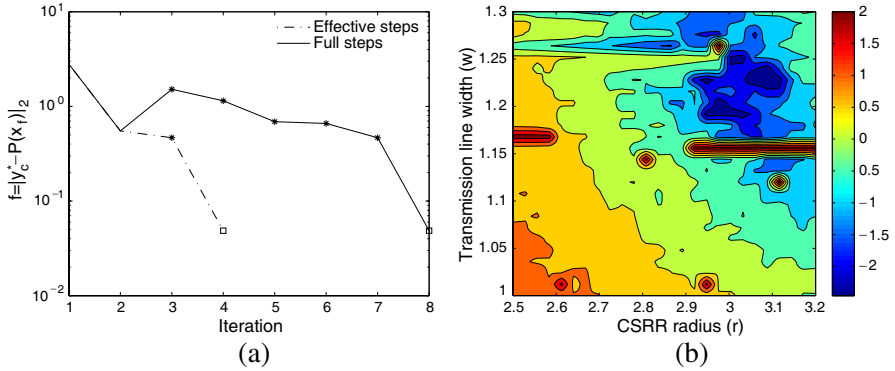


Figure 6. (a) Model-trust space iteration illustrating both the objective function values before and after refinement and (b) the contour plot of the log (objective function values) over a range of r and w values using the optimum values for c and d .

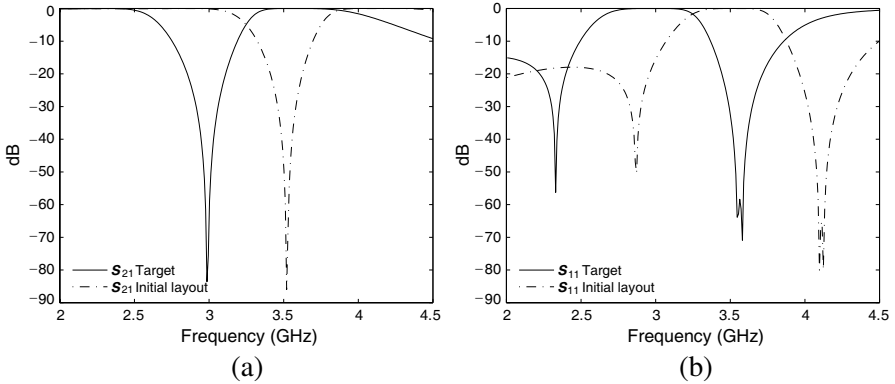


Figure 7. (a) Transmission and reflection (b) coefficient for the initial and final solution of a two-unit periodic CSRR-loaded transmission line.

and quasi-Newton direction in a controlled manner. Coupled with provisions to deal with complex situations, where the step bound may need to contract and then expand based on the representation of the quadratic model, the ASM with model-trust space optimisation provides an effective algorithm for the automatic synthesis of planar microwave structures.

Justification for the need for an effective automated synthesis approach is evident in Figure 7, which shows the comparison between the initial ($P(\mathbf{x}_f^1) = [L_c = 13.61, C_c = 0.15, L = 3.74, C = 1.20]$) and

final response ($P(\mathbf{x}_f^8) = [L_c = 10.88, C_c = 0.29, L = 4.22, C = 1.54]$). This figure clearly illustrates the discrepancies between the initial estimation of the geometric parameters and the final optimised values $\mathbf{x}_f^8 = [r = 3.0 \text{ mm}, d = 0.26 \text{ mm}, w = 1.21 \text{ mm}, c = 0.22 \text{ mm}]$.

5. CONCLUSIONS

In this paper, we presented a novel and efficient automated implementation of an ASM synthesis approach for planar metamaterial structures. Built on a Matlab inspired ASM platform with a fully intergraded VBA controlled EM solver suite, this ASM approach yields satisfactory results after only a few fine model evaluations. Thus eliminating the computational expense of direct optimisation of the high-fidelity full-wave EM model. At the core of this approach is a quasi-Newton model-trust region optimisation algorithm that provides the robustness required to implement an ASM process by combining the global convergence properties of steepest-descent and the fast local convergence of quasi-Newton's methods. The validity of this approach was confirmed by comparing modified and unmodified versions of the quasi-Newton method within the ASM framework, with the model-trust region method clearly outperforming both versions of the quasi-Newton approaches. In both case studies the ASM, with model-trust space optimisation, provides a robust and versatile platform for the automatic synthesis of planar microwave structures.

APPENDIX A. AGGRESSIVE SPACE MAPPING WITH MODEL-TRUST REGION ALGORITHM

begin ASM with Model-trust region

while $\|\mathbf{r}_k\|_2 > tol$

call[$\mathbf{s}, \delta, newton$] \leftarrow Double Dogleg ($newx, \mathbf{J}, \mathbf{r}_k, \delta$)

$\mathbf{x}_{k+1} \leftarrow (\mathbf{x}_k + \mathbf{s})$

if ($\mathbf{x}_{k+1} < \mathbf{x}_{min}$ **or** $\mathbf{x}_{k+1} > \mathbf{x}_{max}$) **then constrain** \mathbf{x}_{k+1} **endif**

while $(\mathbf{x}_{k+1} - \mathbf{x}_k) < 0.01$ **then** $\mathbf{x}_{k+1} \leftarrow (\mathbf{x}_{k+1} + \mathbf{s})$ **endwhile**

simulate $[\omega_z, \omega_p, \omega_0, Z_0] \leftarrow$ Model(\mathbf{x}_{k+1})

$L_c \leftarrow - (L\omega_p^2 (\omega_p^2 - \omega_z^2)) / ((\omega_0^2 - \omega_p^2) (\omega_0^2 - \omega_z^2))$

```

 $C_c \leftarrow 1/(\omega_0^2 L_c)$ ,  $\mathbf{y}_f \leftarrow [L_c; C_c; L; C]$ ,  $\mathbf{r}_{k+1} \leftarrow (\mathbf{y}_c^* - \mathbf{y}_f)$ 
 $ared \leftarrow (\|\mathbf{r}_{k+1}\|_2 - \|\mathbf{r}_k\|_2)$ ,  $slope \leftarrow (\mathbf{J}\mathbf{r}_k)^T \mathbf{s}$ 
if  $ared \geq \alpha * slope$  then
   $\lambda \leftarrow -slope / (2(ared - slope))$ 
  if  $retcode = 3$  then
     $\delta \leftarrow 0.5\delta$ ,  $retcode \leftarrow 0$ ,  $newx \leftarrow \mathbf{true}$ ,  $\mathbf{x}_{k+1} \leftarrow \mathbf{x}_k$ ,  $\mathbf{r}_{k+1} \leftarrow \mathbf{r}_k$ 
  else
     $newx \leftarrow \mathbf{false}$ ,  $retcode \leftarrow 2$ 
    if  $\lambda < 0.1\delta$  then  $\delta \leftarrow 0.1\delta$ 
    elseif  $\lambda > 0.5\delta$  then  $\delta \leftarrow 0.5\delta$ 
    else  $\delta \leftarrow \lambda$ 
    endif
  endif
else
   $pred \leftarrow slope + 0.5\mathbf{s}^T (\mathbf{J}^T \mathbf{J}) \mathbf{s}$ 
  if  $retcode \neq 2$  and  $(\|pred - ared\|_2 \leq 0.1\|ared\|_2)$ 
  or  $ared \leq slope$ 
    and  $newton = \mathbf{false}$ 
     $newx \leftarrow \mathbf{false}$ ,  $retcode \leftarrow 3$ ,  $\mathbf{x}_{k+1} \leftarrow \mathbf{x}_k$ ,  $\mathbf{r}_{k+1} \leftarrow \mathbf{r}_k$ ,
     $\delta \leftarrow 2\delta$ 
  else
     $newx \leftarrow \mathbf{true}$ ,  $retcode = 0$ 
    if  $ared \geq 0.1pred$  then  $\delta \leftarrow 0.5\delta$ 
    elseif  $ared \leq 0.75pred$  then  $\delta \leftarrow 2\delta$ 
    else  $\delta \leftarrow \delta$  endif
  endif
endif
if  $newx = \mathbf{true}$  then
   $\mathbf{J} = \mathbf{J} + (\mathbf{r}_{k+1}\mathbf{s}^T) / (\mathbf{s}^T \mathbf{s})$ ,  $k = k + 1$ 
endif
endwhile
end ASM with Model-trust region

begin Double Dogleg

```

```

if newx then
   $\lambda \leftarrow (\|\mathbf{J}^T \mathbf{r}_c\|_2^2) / \left( (\mathbf{J}^T \mathbf{r}_c)^T (\mathbf{J}^T \mathbf{J}) \mathbf{J}^T \mathbf{r}_c \right), \mathbf{s}^c \leftarrow -\lambda \mathbf{J}_c^T \mathbf{r}_c,$ 
   $\mathbf{s}^n \leftarrow -\mathbf{J}^{-1} \mathbf{r}_c$ 
   $\gamma \leftarrow \lambda \left( (\|\mathbf{J}^T \mathbf{r}_c\|_2^2)^2 / \left( (\mathbf{J}^T \mathbf{r})^T (\mathbf{J}^T \mathbf{J})^{-1} \mathbf{J}^T \mathbf{r}_c \right) \right),$ 
   $\eta \leftarrow 0.8 \|\gamma\|_2 + 0.2$ 
endif
if  $\|\mathbf{s}^n\|_2 \leq \delta$  then
  newton  $\leftarrow$  true,  $\mathbf{s} \leftarrow \mathbf{s}^n$ ,  $\delta \leftarrow \|\mathbf{s}\|_2$ , return
else newton  $\leftarrow$  false
endif
if  $\eta \|\mathbf{s}^n\|_2 \leq \delta$  then  $\mathbf{s} \leftarrow \delta / \|\mathbf{s}^n\|_2$ , return
else if  $\|\mathbf{s}^c\|_2 \geq \delta$  then  $\mathbf{s} \leftarrow \delta / \|\mathbf{s}^c\|_2$ , return
else  $\mathbf{s} \leftarrow \mathbf{s}^c + \tau (\eta \mathbf{s}^n - \mathbf{s}^c)$ , where  $\tau$  is the largest value in  $[0, 1]$ 
  such that  $\|\mathbf{s}\|_2 \leq \delta$ 
endif
end Double Dogleg

```

REFERENCES

1. Bandler, J. W., R. M. Biernacki, S. H. Chen, P. A. Grobelny, and R. H. Hemmers, "Space mapping technique for electromagnetic optimization," *IEEE Transactions on Microwave Theory and Techniques*, Vol. 42, No. 12, 2536–2544, Dec. 1994.
2. Koziel, S., Q. S. Cheng, and J. W. Bandler, "Rapid design optimisation of microwave structures through automated tuning space mapping," *IET Microwaves, Antennas Propagation*, Vol. 4, No. 11, 1892–1902, Nov. 2010.
3. Koziel, S., J. W. Bandler, and Q. S. Cheng, "Robust trust-region space-mapping algorithms for microwave design optimization," *IEEE Transactions on Microwave Theory and Techniques*, Vol. 58, No. 8, 2166–2174, Aug. 2010.
4. Bandler, J. W., R. M. Biernacki, S. H. Chen, R. H. Hemmers, and K. Madsen, "Electromagnetic optimization exploiting aggressive space mapping," *IEEE Transactions on Microwave Theory and Techniques*, Vol. 43, No. 12, 2874–2882, Dec. 1995.
5. Nocedal, J. and S. J. Wright, *Numerical Optimization*, Springer, Aug. 2000.
6. Pawlowski, R. P., J. P. Simonis, H. F. Walker, and J. N. Shadid,

- “Inexact newton dogleg methods,” *SIAM J. Numer. Anal.*, Vol. 46, No. 4, 2112–2132, May 2008.
7. Bakr, M. H., J. W. Bandler, R. Biernacki, S. Chen, and K. Madsen, “A trust region aggressive space mapping algorithm for em optimization,” *IEEE Transactions on Microwave Theory and Techniques*, Vol. 46, 2412–2425, 1998.
 8. Selga, J., A. Rodriguez, M. Gil, J. Carbonell, V. E. Boria, and F. Martin, “Towards the automatic layout synthesis in resonant-type metamaterial transmission lines,” *IET Microwaves, Antennas Propagation*, Vol. 4, No. 8, 1007–1015, Aug. 2010.
 9. Bonache, J., M. Gil, I. Gil, J. Garcia-Garcia, and F. Martin, “On the electrical characteristics of complementary metamaterial resonators,” *IEEE Microwave and Wireless Components Letters*, Vol. 16, No. 10, 543–545, Oct. 2006.
 10. Gil, I., J. Bonache, M. Gil, J. García-García, F. Martín, and R. Marqués, “Accurate circuit analysis of resonant-type left handed transmission lines with inter-resonator coupling,” *Journal of Applied Physics*, Vol. 100, No. 7, 074908, 2006.
 11. Hu, X., Q. Zhang, Z. Lin, and S. He, “Equivalent circuit of complementary split-ring resonator loaded transmission line,” *Microwave and Optical Technology Letters*, Vol. 51, No. 10, 2432–2434, 2009.
 12. Caloz, C. and T. Itoh, *Electromagnetic Metamaterials: Transmission Line Theory and Microwave Applications*, Wiley, 2005.
 13. Pozar, D. M., *Microwave Engineering*, 3rd Edition, Wiley, 2005.
 14. Baena, J. D., J. Bonache, F. Martin, R. M. Sillero, F. Falcone, T. Lopetegui, M. A. G. Laso, J. Garcia-Garcia, I. Gil, M. F. Portillo, and M. Sorolla, “Equivalent-circuit models for split-ring resonators and complementary split-ring resonators coupled to planar transmission lines,” *IEEE Transactions on Microwave Theory and Techniques*, Vol. 53, No. 4, 1451–1461, Apr. 2005.
 15. Bahl, I. J. and P. Bhartia, *Microwave Solid State Circuit Design*, Wiley-Interscience, 2003.
 16. Vicente, L. N., “Space mapping: Models, sensitivities, and trustregions methods,” *Optimization and Engineering*, Vol. 4, 159–175, 2003.
 17. Dennis, Jr., J. E. and R. B. Schnabel, *Numerical Methods for Unconstrained Optimization and Nonlinear Equations (Classics in Applied Mathematics)*, Vol. 16, Society for Industrial & Applied Mathematics, 1996.

18. Powell, M. J. D., "A hybrid method for nonlinear equations," *Numerical Methods for Nonlinear Algebraic Equations*, Philip Rabinowitz, Ed., 87–114, Gordon & Breach, 1970.
19. Dennis, J. E. and H. H. W. Mei, "Two new unconstrained optimization algorithms which use function and gradient values," *Journal of Optimization Theory and Applications*, Vol. 28, 453–482, 1979.
20. Bonache, J., M. Gil, O. Garca-Abad, and F. Martn, "Parametric analysis of microstrip lines loaded with complementary split ring resonators," *Microwave and Optical Technology Letters*, Vol. 50, No. 8, 2093–2096, Aug. 2008.